Baseline Demographics	
Number of patients	11
Age	
Median (IQR)	37(21)
Sex	
Female	7
Male	4
Pretreatment Medications	
Anticonvulsant	4
Benzodiazepine	3
Selective GABA-BZ1 agonist	1
SSRI	5
SNRI	4
Tricyclic antidepressant	1
Serotonin modulator	5
Bupropion	1
Alpha-2 agonist	1
Stimulant	3
Typical antipsychotic	1
Atypical antipsychotic	7
Lithium Carbonate	1
Triptan	1

Supplemental Table 1. Baseline patient demographics.

Participant	Condition					Total CPCs
	DT	Week 1		Week 2		
	E	E	K	E	K	
1131	84	140	93	131	70	518
1132	144	237	112	131		624
1133	485	149	114	126	111	985
1135		12	36	12	36	96
1137	120	115	162	53	273	723
1138		438	358	293	173	1262
1139	40	90	73	90	86	379
1140	462	405	103	231	110	1311
1144	95	98	117	122	129	561
1145	77	57	65			199
1147	47	96	43	20	64	270
Total CPCs	1554	1837	1276	1209	1052	6928

Supplemental Table 2. CPC incidence across seizures. Table depicting number of CPCs for each seizure across all participants, organised by seizures induced during dose charge titration (DT) sessions, etomidate (E), or ketamine (K) during week 1 or week 2. The column labelled "Total CPCs" indicates the total number of complexes detected from each individual throughout their experimental treatment course. Grey cells indicate sessions where recordings did not occur.

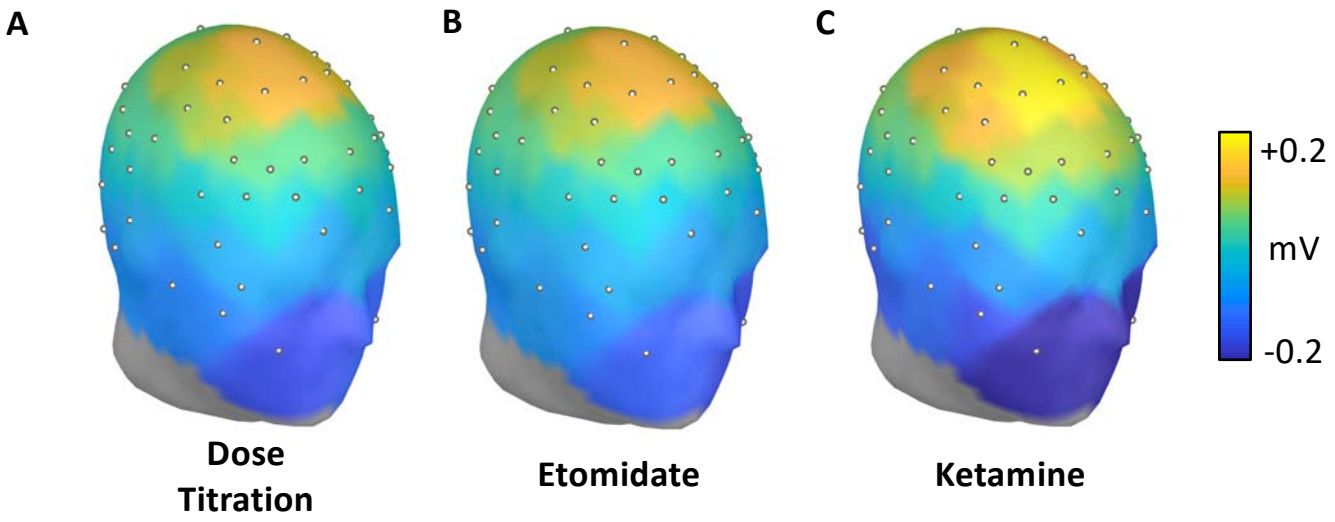

Supplemental Figure 1. Invariance of average peak CPC scalp topologies across stimulation dose charge and anaesthetic regimen. **(A)** Initial dose-charge titration session with etomidate general anaesthesia. **(B)** ECT with etomidate general anaesthesia. **(C)**. ECT with ketamine general anaesthesia.

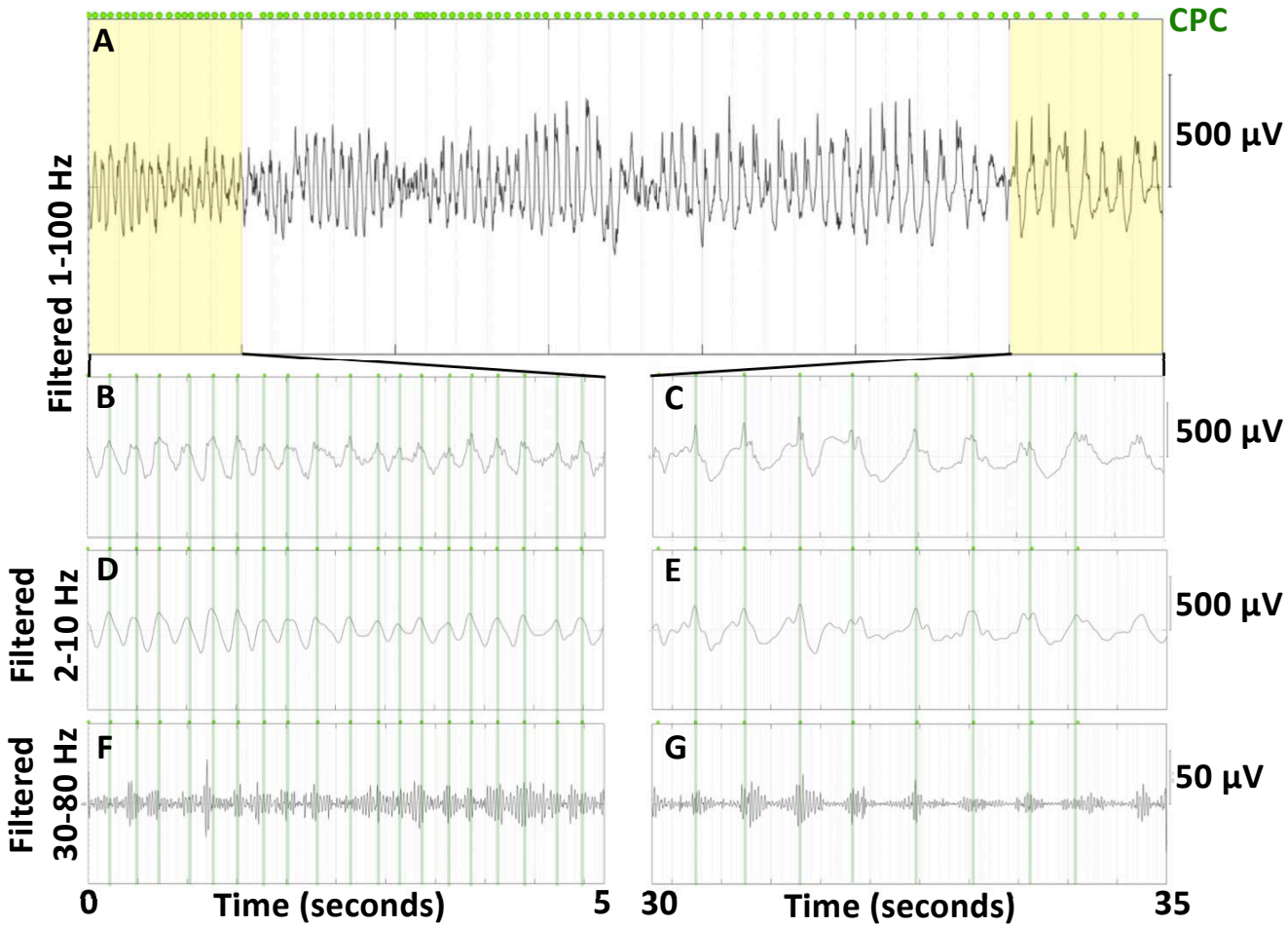

Supplemental Figure 2. Gamma band oscillations associated with CPCs. **(A)** CPCs were detected (green dots) during the course of Phase III using Cz-Facial average signals. Initial and final 5 second intervals (yellow regions) are shown in greater detail in **(B-C)** with times of CPC peak amplitude (green vertical lines). **(D-E)** CPCs are apparent using 2-10 Hz bandpass filtering of the EEG. **(F-G)** With 30-80 Hz bandpass filtering, gamma-band oscillations associated with CPCs are evident.

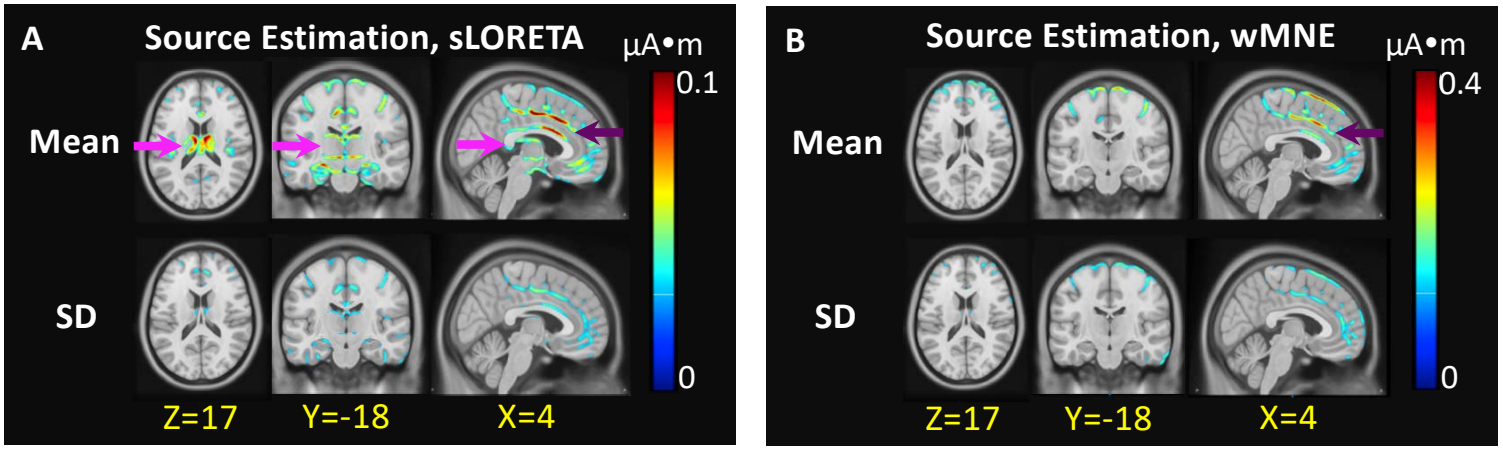

Supplemental Figure 3. Consistency of CPC source estimation. Generic head models were utilized to localize neural sources of CPC peak positive EEG activity to surfaces of the cortex, hippocampus, and thalamus. These source esimations were averaged across all sessions and individuals. (**A)** Through standardized low resolution electromagnetic tomography (sLORETA), CPC source estimation converged most strongly to cingulate cortical regions (purple arrow) and superficial thalamic (magenta arrows) regions. (**B)** Using weighted minimum norm estimation (wMNE), current density mapping identified cingulate cortical regions (purple arrow) in addition to superficial frontal and parietal regions.

Supplemental Video. Consistency of CPC topology and source localization during one seizure. Video illustrating the topology and source localization of each CPC for an entire seizure. A single channel EEG trace representing CPCs for the entire seizure in the bottom panel, with green circles above the EEG trace marking each CPC. The traveling red line marks sequential CPCs, with simultaneous projection of topographic surface maps (upper left panel) and dSPM source estimation projected to anatomic surfaces (upper right panel). CPCs consistently demonstrate maximal positive amplitude over the vertex and negative amplitude over suborbital region, while dSPM shows localization to the midline thalamus and cingulate regions.